Accepted Manuscript

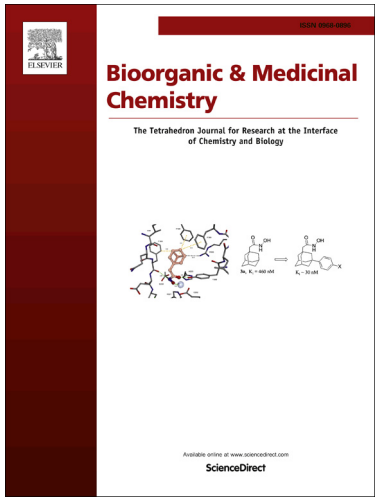

New pyridin-3-ylmethyl carbamodithioic esters activate pyruvate kinase M2 and potential anticancer lead compounds

Yu Zhang, Bin Liu, Xingyu Wu, Ridong Li, Xianling Ning, Yu Liu, Zhenming Liu, Zemei Ge, Runtao Li, Yuxin Yin

PII: S0968-0896(15)00451-4
DOI: http://dx.doi.org/10.1016/j.bmc.2015.05.041
Reference: BMC 12337

To appear in: *Bioorganic & Medicinal Chemistry*

Received Date: 1 April 2015
Revised Date: 18 May 2015
Accepted Date: 20 May 2015

Please cite this article as: Zhang, Y., Liu, B., Wu, X., Li, R., Ning, X., Liu, Y., Liu, Z., Ge, Z., Li, R., Yin, Y., New pyridin-3-ylmethyl carbamodithioic esters activate pyruvate kinase M2 and potential anticancer lead compounds, *Bioorganic & Medicinal Chemistry* (2015), doi: http://dx.doi.org/10.1016/j.bmc.2015.05.041

This is a PDF file of an unedited manuscript that has been accepted for publication. As a service to our customers we are providing this early version of the manuscript. The manuscript will undergo copyediting, typesetting, and review of the resulting proof before it is published in its final form. Please note that during the production process errors may be discovered which could affect the content, and all legal disclaimers that apply to the journal pertain.

ACCEPTED MANUSCRIPT

Graphical Abstract

To create your abstract, type over the instructions in the template box below.
Fonts or abstract dimensions should not be changed or altered.

New pyridin-3-ylmethyl carbamodithioic esters activate pyruvate kinase M2 and potential anticancer lead compounds

Leave this area blank for abstract info.

Yu Zhang [a, †], Bin Liu [b, †], Xingyu Wu [a], Ridong Li [a, b], Xianling Ning [a], Yu Liu [a], Zhenming Liu [b], Zemei Ge [b], Runtao Li [b, *], Yuxin Yin [a, b, *]

[a] *Institute of Systems Biomedicine, Department of Pathology, School of Basic Medical Sciences, Beijing Key Laboratory of Tumor Systems Biology, Peking University Health Science Center, Beijing 100191, China.*

[b] *State Key Laboratory of Natural and Biomimetic Drugs, Peking University, Beijing 100191, China.*

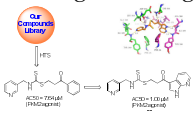

ACCEPTED MANUSCRIPT

ACCEPTED MANUSCRIPT

Bioorganic & Medicinal Chemistry
journal homepage: www.elsevier.com

New pyridin-3-ylmethyl carbamodithioic esters activate pyruvate kinase M2 and potential anticancer lead compounds

Yu Zhang [a, †], Bin Liu [b, †], Xingyu Wu [a], Ridong Li [a, b], Xianling Ning [a], Yu Liu [a], Zhenming Liu [b], Zemei Ge [b], Runtao Li [b, *], Yuxin Yin [a, b, *]

[a] *Institute of Systems Biomedicine, Department of Pathology, School of Basic Medical Sciences, Beijing Key Laboratory of Tumor Systems Biology, Peking University Health Science Center, Beijing 100191, China.*
[b] *State Key Laboratory of Natural and Biomimetic Drugs, Peking University, Beijing 100191, China.*
[†] *These authors contributed equally.*

ARTICLE INFO

Article history:
Received
Received in revised form
Accepted
Available online

Keywords:
Pyruvate kinase M2
Dithiocarbamic acid ester
Structure-activity relationship
Anti-proliferation
Docking

ABSTRACT

Pyruvate Kinase M2 (PKM2) is a key protein responsible for cancer's Warburg effect. Activation of PKM2 may alter aberrant metabolism in cancer cells, which suggests PKM2 as a tumor selective therapeutic target. In this paper, the lead compound **8** was first discovered as a new kind of PKM2 activator from a random screening of an in-house compound library. Then, a series of lead compound **8** analogues were designed, synthesized and evaluated for their activation of PKM2 and anticancer activities. 7-Azaindole analogue **32** was identified as the most potent PKM2 activator. Compounds with potent enzyme activity also exhibited selective anti-proliferation activity on cancer cell lines HCT116, Hela and H1299 compared with non-tumor cell line BEAS-2B. The structure-activity relationships of these compounds were supported by molecular docking results. Preliminary pharmacological studies also showed that compound **32** arrests the cell cycle at the G2/M phase in HCT116 cell line.

2009 Elsevier Ltd. All rights reserved.

1. Introduction

One of the most important distinctions between healthy and cancerous tissues was the difference in metabolism. In normal cells, glycolysis is induced by hypoxia. Cancer cells, however, preferentially metabolize glucose by glycolysis, even in an aerobic environment. The phenomenon is known as Warburg effect.[1, 2] Pyruvate kinase (PK), a key enzyme that catalyzes the last step of glycolysis is considered to be responsible for such metabolic alteration.[3]

PK is a tetrameric enzyme encoded by four isozymes (PKL, PKR, PKM1, and PKM2) that differ in their kinetic properties and tissue distributions.[4-7] PKL and PKR are encoded by the same gene PKLR but under the control of different tissue-specific promoters. The two isoforms are expressed in liver and red blood cells, respectively.[7] Most tissues express either PKM1 or PKM2 isoform. PKM1 is expressed in normal differentiated tissues; whereas PKM2 is predominantly found in highly proliferating cells including cancer cell lines and tumors.[5] PKM1 and PKM2 are two different splicing forms of the same mRNA transcribed from the PKM gene.[6]

Despite their similarity in primary sequences, PKM1 and PKM2 have different catalytic and regulatory properties. PKM1 has constitutively high enzyme activity. In contrast, PKM2 requires activation by the binding of fructose-1, 6-bis-phosphate (FBP) at an allosteric site. Additionally, PKM2 can interact with proteins harboring phosphorylated tyrosine residues, leading to the release of FBP, which, in turn, reduces the activity of the enzyme.[8] Thus, most of PKM2 exists as less active forms with low catalytic rate in tumors.[9] In cancer cells, independently of their tissue of origin PKM2 gradually replaces the tissue-specific PK isoform and becomes a predominant isoform.[10] This interesting phenomenon has raised the question of how PKM2 expression benefits tumor cells.

One hypothesis is that low PKM2 activity facilitating the flux of glucose carbons into the anabolic pathways help meet cancer cells' need for biological building blocks to support the production of new cells.[11] Cancer cells' favor for the low activity of PKM2 isoform was further supported by the fact that replacement of PKM2 with constitutively active PKM1 inhibits xenograft tumor.[12] Furthermore, the PKM2 form with low activity can translocate to cell nucleus under certain

* Corresponding author. E-mail: lirt@bjmu.edu.cn, (R. Li).
* Corresponding author. E-mail: yinyuxin@hsc.pku.edu.cn, (Y. Yin).

ACCEPTED MANUSCRIPT

circumstance, which can subsequently increases the expression of c-Myc, GLUT1, LDHA, PTB and PKM2 itself, thereby promoting the Warburg effect and tumorigenesis.[13-16] High expression of PKM2 in cancer and its low activity form of tumorigenic function suggest that activating PKM2 is a therapeutic strategy for cancer.

Several categories of PKM2 activators (Fig. 1) have been reported including a series of N,N'-diarylsulfonamides (**1**),[17] thieno[3,2-b]pyrrole[3,2-d]pyridazinones (**2**),[18] 2-oxo-N-aryl-1,2,3,4-tetrahydroquinoline-6-sulfonamides (**3**),[19] quinolone sulfonamides (**4**),[20] 1-(sulfonyl)-5-(arylsulfonyl)indoline (**5**),[21] 2-((1H-benzo[d]imidazol-1-yl)methyl)-4H-pyrido[1,2-a]pyrimidin-4-ones (**6**)[22] and 3-(trifluoromethyl)-1H-pyrazole-5-carboxamide (**7**).[23] Even though, the above compounds have no anti-proliferative effects on tumor cell lines except that serine was deprived from the medium. In this article, we describe the discovery of new kinds of dithiocarbamatic acid esters as PKM2 selective activators with significant anti-proliferative effects on tumor cell lines.

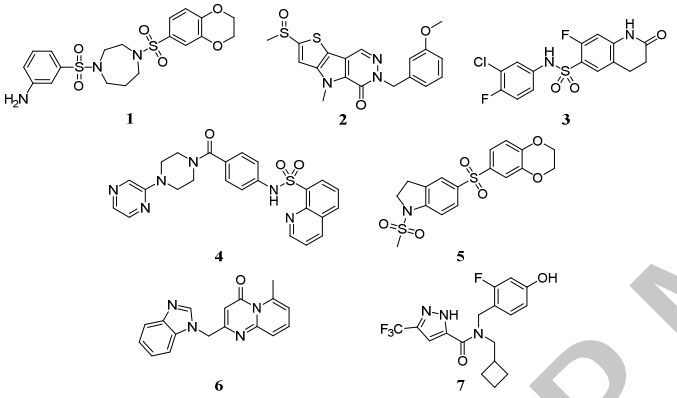

Fig. 1. Several categories of PKM2 activators.

2. Results and discussion

2.1. Chemistry

On the basis of our established PKM2 model, the lead compound **8** (AC_{50} = 7.64 μM), a new kind of PKM2 activator, was identified from a random screening of an in-house compound library (~ 1000 total). Our previous study has showed that the pyridin-3-ylmethanamine moiety of compound **8** is crucial for antitumor activity.[24] Therefore, in order to further improve the activity, we focused our attention on the modification of phenyl ketone of compound **8**, which was replaced with various aryl or heterocyclic ketones (Fig. 2).

The synthesis of compounds **9-35** is depicted in Scheme 1. Various aryl or hetroaryl ketones reacted respectively with paraformaldehyde catalyzed by diisopropylammonium trifluoroacetate to form the intermediates acryloyl arenes,[25] which were followed by the addition of dithiocarbamates from CS_2 and 3-(aminomethyl)pyridine to afford the corresponding target compounds **9-35**.[26] Most of the starting materials, acetyl arenes, are commercially available except that of compounds **32-34.** Their starting materials were prepared according to the literatures.[27,28]

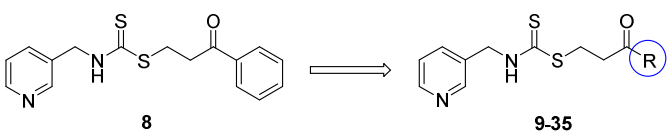

Compd.	R	Compd.	R
8	Ph	**22**	3,4,5-trimethoxy
9	4-ClPh	**23**	2-naphthalene
10	4-FPh	**24**	1-naphthalene
11	4-OHPh	**25**	2-furan
12	4-CNPh	**26**	2-thiophene
13	4-NO_2Ph	**27**	2-pyrrole
14	4-$(CH_3)_2$NPh	**28**	2-thiazole
15	4-BnOPh	**29**	3-pyridine
16	4-OMePh	**30**	3-coumarin
17	4-CF_3Ph	**31**	3-indole
18	2-OMePh	**32**	3-azaindole
19	2-ClPh	**33**	3-imidazo[1,2-a]pyridine
20	3,4-dichloro	**34**	PhCH=CH
21	3,4-difluo	**35**	3-pyrrole

Fig. 2. Lead compound **8** and strategy for its structural modification

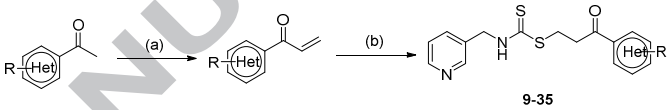

Scheme 1. Synthesis of compounds **8-35**. Reagents and conditions: (a) $(HCHO)_n$, $CF_3COOH{\cdot}(iPr)_2NH$, DMF, 90 °C, 24 h; (b) 3-(aminomethyl)pyridine, CS_2, TEA, DMF, rt, 12 h.

2.2. Biological evaluations in vitro

The cell-free enzymatic assay of PKM2 activity was performed as described in Experiment Section. All the target compounds were subjected to this assay to evaluate their affinity toward isolated PKM2 kinase. It is clear that a slight change of aryl group in compound **8** could induce obviously influence on the activity (Table 1). The introduction of the *para*-substitutents, including electron withdrawing or donating groups, on the benzene ring of compound **8** led to the decrease of activity or opposite activities (**9**, **10**, **14**, **17**, **20**-**22**). However, NO_2 or CN substituted derivatives (**12**, AC_{50} = 4.39 μM; **13**, AC_{50} = 2.76 μM) showed 2-3 fold increase of activities compared with lead compound **8**, which could be explained by the function of hydrogen bond receptor of them. Notably, when the benzene ring in compound **8** was replaced with the heterocycles, we observed the similar trend that only the heterocyle derivatives containing hydrogen bond receptor (**25**, **28**, **29**, **32**) showed remarkable activities (AC_{50} = 4.30, 3.56, 3.70, 1.00 μM). More interestingly, the activity of the azaindole derivatives **32** (AC_{50} = 1.00 μM) is greatly higher than that of indole derivatives **31** (AC_{50} > 20 μM). A feasible explanation for this phenomenon may be due to the interaction of N atom in azaindole with other residues of the PKM2 receptor, which is further discussed in docking studies later. It was also found that *ortho*-substitution is more favorable for the activity than *para*-substitution, such as, compounds **16** (*4*-OMe, AC_{50} = 11.18 μM) and **18** (*2*-OMe AC_{50} = 3.93 μM); compounds **9** (*4*-Cl, AC_{50} > 20 μM) and **19** (*2*-Cl, AC_{50} = 5.61 μM). 3-Pyrrole derivatives (**35**, AC_{50} = 4.34 μM) exhibited higher activity than 2-pyrrole derivatives (**27**, AC_{50} > 20 μM), which further demonstrated that the position of substituent was crucial for the activity. Furthermore, replacing the benzene ring in compound **8** with naphthalene ring (**23** and **24**), or introducing

ACCEPTED MANUSCRIPT

multiple substituents (**20**, **21**, **22**) led to the decrease or completely lost of activity, which indicated that larger steric hindrance was unfavorable to the activity.

2.3. Growth inhibitory activity on cancer cell lines

The previous reported compounds have no anti-proliferative effects on tumor cell lines unless serine or glutamate was deprived from the medium.[29] However, our series of PKM2 activators exhibited promising antitumor activity at cellular level.

Table 1. Activity of dithiocarbamic acid esters on PKM2.

Compd.	R	AC_{50}[a] (μM)	Max, (%) Resp[b]
8	Ph	7.64	24
9	4-ClPh	>20	NA
10	4-FPh	9.83	48
11	4-OHPh	6.23	76
12	4-CNPh	4.39	61
13	4-NO_2Ph	2.76	49
14	4-$(CH_3)_2$NPh	inhibit[c]	inhibit[c]
15	4-BnOPh	>20	NA
16	4-OMePh	11.18	63
17	4-CF_3Ph	>20	23
18	2-OMePh	3.93	88
19	2-ClPh	5.61	63
20	3,4-dichloro	inhibit[c]	inhibit[c]
21	3,4-difluo	>20	42
22	3,4,5-trimethoxy	10.13	131
23	2-naphthalene	inhibit[c]	inhibit[c]
24	1-naphthalene	inhibit[c]	inhibit[c]
25	2-furan	4.30	107
26	2-thiophene	>20	29
27	2-pyrrole	>20	126
28	2-thiazole	3.56	72
29	3-pyridine	3.70	106
30	3-coumarin	inhibit[c]	inhibit[c]
31	3-indole	>20	NA
32	3-azaindole	1.00	182
33	3-imidazo[1,2-a]pyridine	18.15	101
34	PhCH=CH	inhibit[c]	inhibit[c]
35	3-pyrrole	4.34	30

[a] AC_{50} values were determined using enzymatic PKM2 activity assay.

[b] %FBP indicates the extent of maximal activation, relative to FBP (normalized to 100%).

[c] Compound inhibits PKM2 activity.

Ten of the compounds, which show potent PKM2 activity, were chosen to examine the anti-proliferative effects in human colon carcinoma cell (HCT116), human cervical carcinoma cell (Hela), and human non-small-cell lung cancer cell (H1299). As no reported PKM2 activators exhibit cellular activity, the antitumor drug Taxol was selected as positive control to test the sensitivity of the model. As shown in Table 2, the result of Taxol was consistent with previous reports,[30,31] confirming the accuracy of our experiment. The IC_{50} values of tested compounds against different tumor cells ranged between 0.64 and 5.6 μM. Among them, Hela cells were the most sensitive to these compounds with most IC_{50} value in the nanomolar range. H1299 cells were the least sensitive to these compounds among these cell lines. In particular, compound **18** showed the greatest anti-proliferation activity towards these cell lines, which is also potent at enzyme level. To further explore the selectivity of these compounds against cancer cells, they were also examined in BEAS-2B cells derived from normal human bronchial epithelial cells. As seen in Table 2, all tested compounds demonstrated high selectivity on cancer cells. These results are consistent with the theory that activating PKM2 is a tumor selective therapeutic strategy as normal cells favor high activity of pyruvate kinase.

Table 2. In vitro cytotoxicity of selected compounds against cancer cell lines and non-tumor cells.

Compd.	IC_{50}[a] (μM)			
	HCT116	Hela	H1299	BEAS-2B
Taxol	0.01	0.0043	0.05	7.38
8	2.00	1.12	4.90	19.04
11	1.86	1.19	4.25	24.40
12	1.81	0.94	4.51	22.56
13	2.80	0.99	3.89	28.11
18	0.64	0.65	3.91	12.11
19	1.53	0.91	3.08	13.08
25	3.66	1.81	4.04	14.95
28	1.90	0.84	3.35	15.81
29	2.39	0.85	5.56	19.34
32	3.15	1.12	4.24	21.59

[a] The anti-proliferative activities of selected compounds to tumor cells were determined by the MTT assay.

2.4. Selectivity on other isoforms of pyruvate kinase

An effective antitumor agent targeting tumor specific PKM requires a high degree of selective activation of PKM2 relative to other PK targets with particular consideration for PKM1. Thus the compound **32** with the highest activity on PKM2 was chosen to test the selectivity versus other PK isoforms PKM1 and PKR. As shown in Figure 3, compound **32** has no significant activity on PKR and PKM1.

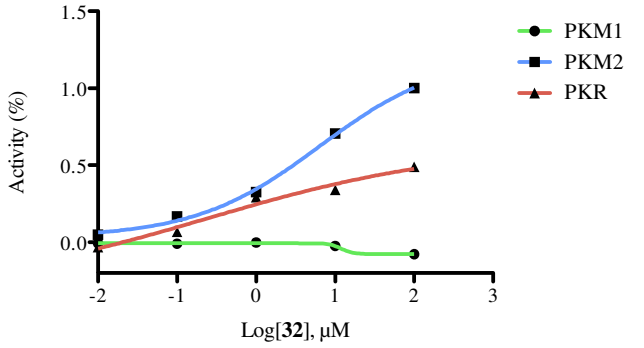

Fig. 3. Selectivity assessment for **32** versus PKM2(■), PKM1(●), PKR(▲). Maximum activation of PKM2 was normalized to 100%.

2.5. Effect on cell cycle by Flow Cytometry

ACCEPTED MANUSCRIPT

The compound **32** was also selected to be further studied regarding to its effects on cell cycle progression. Exposure of HCT116 cells to compound **32** resulted in an interference with normal cell cycle distribution of this cell line. As illustrated in Figure 4, the treatment of **32** caused blockage of the cell cycle in the G2/M phase. Compared with control cells treated with DMSO, when HCT116 cells were treated with increasing concentrations of **32** (1 μM, 5 μM), the mean percentage of cells in the G2/M phase increased from 22.74 % to 59.75 %, and the percentages of cells in S and G0/G1 phase decreased concomitantly (Fig. 4). The result is consistent with the report that nuclear PKM2 is required for cell division by interacting with Bub3, MCL2 in brain tumors.[32,33] Our results suggest that this series of compounds may exhibit antitumor activity by preventing PKM2 from entering nucleus.

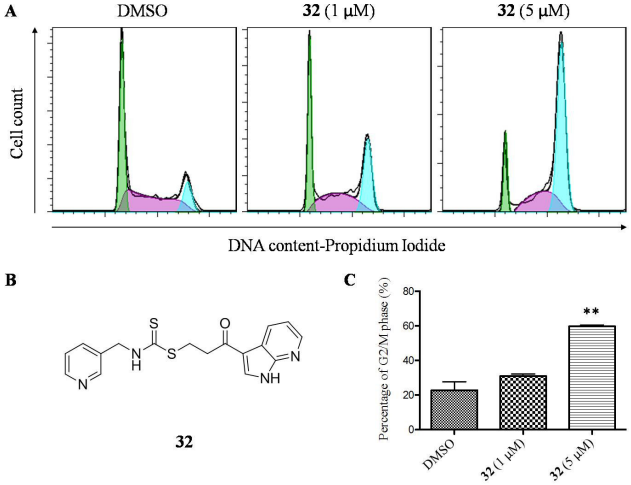

Fig. 4. Compound **32** blocked cell cycle. (A) Compound **32** dose-dependent induced cell cycle arrest in G2/M phase of HCT116 cells. (B) The structure of compound **32**. (C) The profiles showed the proportions (%) in G2/M phase of HCT116 cells treated with **32** and diluent (DMSO). The experiments were repeated three times, and a representative experiment is shown: (***) $p < 0.001$ compared to control.

2.6. Docking studies and structure–activity relationship discussion

To get further insight into the binding profile and reveal the structure-activity relationship of the newly synthesized compounds, a docking study of compound **32** with PKM2 was carried out. The binding mode of compound **32** in the activator pocket of PKM2 is shown in Figure 5.

From Figure 5 (D), our results demonstrated that compound **32** binds into the pocket with an overall binding affinity of -9.28 kcal/mol, and shares a similar binding mode with compound **4** (NZT). From Figure 5 (A) and (B), the active hydrogen on 7-azaindole forms a strong hydrogen bond with Ala388C, while the 7-nitrogen serves as a hydrogen bond acceptor to bind with Tyr390C. The carbonyl group of the compound is found to be engaged in a hydrogen bonding with the positively charged side chain of Lys311D, which highly simulates the function of the same group of the original ligand. The active hydrogen from the dithiocarbamic acid ester group contributes to another hydrogen bond with Leu353D. Furthermore, a valid polar contact is found between the nitrogen on the pyridine plane and Tyr390D. Two pairs of pi-pi stacking interactions are present between the 7-azaindole group and Phe26C, and also the pyridine group and Phe26D.

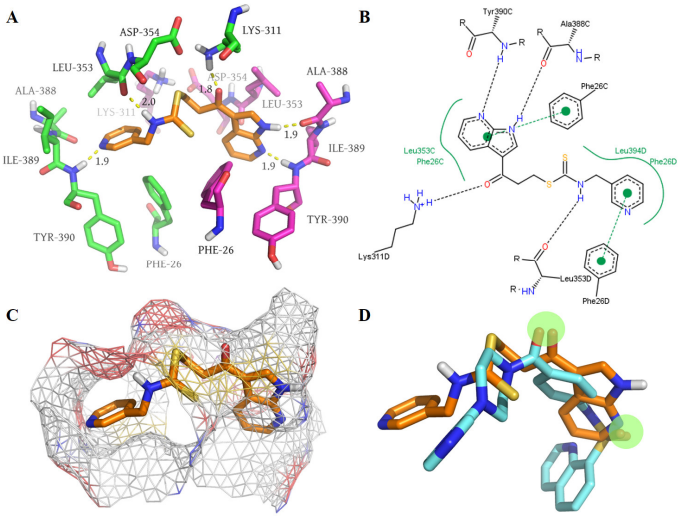

Fig. 5. The binding profile of compound **32** with the activator pocket of PKM2. (A) 3D binding plot: compound **32**, residues of chain C and chain D of the receptor are colored orange, purple and green respectively. Yellow dashes indicate hydrogen bonds or polar contacts, while the number to the next demonstrates the distance of the interaction. (B) 2D binding plot: black dashes, green dashes and green curves correspondingly indicate hydrogen bonds, pi-pi stacking and hydrophobic interactions. (C) Surface plot: surface (shown as grids) of residues which are within 12 Å of the compound. Blue, red and yellow grids represents nitrogen, oxygen and sulfur atoms respectively. (D) Alignment plot: compound **32** is aligned with the original ligand (cyan sticks) from the receptor (PDB ID: 4G1N, ligand: NZT) in its crystallized conformation within the binding site. Transparent green circles highlighted the highly similar features of both molecules.

According to the docking results and the AC_{50} of compound **27** and **32**, we hypothesized that a hydrogen bond donor (on a five-membered ring) is expected to be present at γ-site of the ketone so as to form a hydrogen bonding with Ala388C. If this is the case, the low binding affinity (-7.82 kcal/mol) and activity of 2-pyrrole substitution can be attributed to its improper position of the hydrogen bond donor. To validate it, compound **35** with a 3-pyrrole substitution is synthesized. As expected, a significant increase of AC_{50} has been observed from compound **27** to **35**, which in turn confirm the reliability of the docking results. The introduction of other rings could always decrease the activity and lead to an unfavorable curled conformation (see Supplementary Information, Fig. S1.), which can be seen in compounds **23, 24, 31** and **33**. But in the case of compound **32**, the 7-nitrogen of the azaindole group is elegantly positioned right at almost the same coordinate of sulfanilamide oxygen atom of NZT. Except for adding a necessary hydrogen bond as an acceptor, it also fixes the azaindole plane in such a way that Phe26C could easily form a pi-pi stacking interaction with it.

In this section, we found that compound **32** has a relatively good binding profile within PKM2's activator pocket. Predictions from the docking results correspond to the bioassay results, making the simulation model reliable and useful for further compound modifications.

3. Conclusion

In this report, the lead compound **8** was identified as a PKM2 activator from a random screening of an in-house compound

ACCEPTED MANUSCRIPT

library. To explore the SAR and get more potent compounds, a series of compound **8** analogs were synthesized and biologically evaluated. Most of them functioned as activators of PKM2 and showed potent anti-proliferative activities against HCT116, Hela and H1299 cell lines. The compound **32** was identified as the most potent PKM2 selective activator. The result is supported by molecular docking simulation, which shows that compound **32** nicely fits into the binding pocket. A flow cytometric study was carried out to further explore the biological mechanism of this compound. The result demonstrates that compound **32** delayed cell cycle progression by arresting cells in G2/M phase, which may be due to the compounds' preventing PKM2 from entering nucleus. This study provides a new molecular scaffold for further development of antitumor agents that target PKM2.

4. Experimental section

4.1. Materials and methods

Unless otherwise stated, starting materials were purchased from Alfa Aesar, TCI, Energy or Arcos and used without purification. All of the reactions were monitored by thin layer chromatography (TLC) on GF254 silica gel plates.^{1}H NMR spectra and ^{13}C NMR spectra were recorded on a Bruker AVANCE III 400 (400 MHz) spectrometer in needful D-reagents with tetramethylsilane (TMS) as an internal reference. NMR chemical shifts are reported as values (ppm) relative to internal tetramethylsilane and splitting patterns are designated as: s = singlet, d = doublet, t = triplet, q = quartet, m = multiplet. HRMS of additional products were carried out on Brucker Apex IV FTMS. Melting points were measured as uncorrected values.

4.2. Typical procedure for the synthesis of target compounds 8-31 and 35

To a mixture of aryl ketone (5.0 mmol) and paraformaldehyde (10.0 mmol) in DMF 10 mL was added catalyst (ammonium salts) (5.0 mmol). The mixture was vigorously stirred at 90 ^{o}C for 24 h. After that, H_2O (40 mL) was added and then extracted with EtOAc (10 mL × 3), combined organic phase was washed with saturated NaCl (aq) and dried over Na_2SO_4, and then filtered, the solvent was removed under reduced pressure to form the intermediates acryloyl arenes.

A mixture of 3-(aminomethyl)pyridine (5.0 mmol) and TEA (5.0 mmol) in 20 mL DMF/H_2O (10:1) was added CS_2 (0.32 mL). The solution was stirred at room temperature for 30 mins followed by the addition of acryloyl arenes from last step. The resulting mixture was then stirred for 12 h at room temperature. H_2O (40 mL) was added to the reaction mixture, and then it was extracted with EtOAc (20 mL × 3), combined organic phase was washed with saturated NaCl (aq), dried (Na_2SO_4), filtered, the solvent was removed under reduced pressure. The crude product was purified by flash column chromatography on silica gel with a gradient eluent of EtOAc /MeOH and further recrystallized from EtOAc/PET to give crystals of the target compounds.

4.2.1. 3-Oxo-3-phenylpropyl (pyridin-3-ylmethyl)carbamodithioate (8) White solid, m.p. 82.3~84.6 ^{o}C. Yield: 54%. ^{1}H NMR (400 MHz, DMSO-d_6) δ 10.50 (s, 1H), 8.70-8.32 (m, 2H), 7.97 (d, J = 7.4 Hz, 2H), 7.66 (ddd, J = 10.8, 8.5, 4.4 Hz, 2H), 7.53 (t, J = 7.1 Hz, 2H), 7.37 (dd, J = 7.7, 4.8 Hz, 1H), 4.86 (d, J = 5.3 Hz, 2H), 3.50 (dt, J = 11.8, 4.7 Hz, 4H). ^{13}C NMR (100 MHz, DMSO-d_6) δ 198.7, 197.8, 149.5, 148.9, 136.7, 136.0, 133.9, 133.4, 129.3, 128.4, 124.0, 47.6, 38.7, 29.3. Anal. Cald for $C_{16}H_{16}N_2OS_2$: C, 60.73; H, 5.10; N 8.85; Found: C, 60.91; H, 5.16; N, 8.81.

4.2.2. 3-(4-Chlorophenyl)-3-oxopropyl (pyridin-3-ylmethyl)carbamodithioate (9) White solid, m.p. 113.7~113.9 ^{o}C. Yield: 22%. ^{1}H NMR (400 MHz, DMSO-d_6) δ 10.52 (t, J = 5.2 Hz, 1H), 8.77-8.34 (m, 2H), 8.22-7.93 (m, 2H), 7.70 (dt, J = 7.8, 1.8 Hz, 1H), 7.68-7.52 (m, 2H), 7.36 (dd, J = 7.8, 4.8 Hz, 1H), 4.85 (d, J = 5.3 Hz, 2H), 3.62-3.40 (m, 4H). ^{13}C NMR (100 MHz, DMSO-d_6) δ 197.8, 197.7, 149.6, 148.9, 138.8, 136.0, 135.3, 133.4, 130.3, 129.3, 124.0, 47.6, 38.7, 29.2. HRMS Calcd. For $C_{16}H_{16}ClN_2OS_2^+$ [M+H]$^+$ 351.0387, found: 351.0380.

4.2.3. 3-(4-Fluorophenyl)-3-oxopropyl (pyridin-3-ylmethyl)carbamodithioate (10) White solid, m.p. 127.4~128.1 ^{o}C. Yield: 35%. ^{1}H NMR (400 MHz, DMSO-d_6) δ 10.60 (t, J = 5.5 Hz, 1H), 8.81-8.35 (m, 2H), 8.33-7.92 (m, 2H), 7.93-7.56 (m, 1H), 7.46-7.17 (m, 3H), 4.85 (d, J = 5.6 Hz, 2H), 3.72-3.40 (m, 4H). ^{13}C NMR (100 MHz, DMSO-d_6) δ 197.7, 197.3, 166.8, 164.3, 149.6, 148.9, 136.0, 133.4, 131.5, 131.4, 123.9, 116.4, 116.1, 47.5, 45.8, 38.7. HRMS Calcd. For $C_{16}H_{16}FN_2OS_2^+$ [M+H]$^+$ 335.0683, found: 384.0680.

4.2.4. 3-(4-Hydroxyphenyl)-3-oxopropyl (pyridin-3-ylmethyl)carbamodithioate (11) White solid, m.p. 166.7~167.2 ^{o}C. Yield: 11%. ^{1}H NMR (400 MHz, DMSO-d_6) δ 8.75-8.35 (m, 2H), 7.85 (d, J = 8.7 Hz, 2H), 7.81-7.60 (m, 1H), 7.38 (dd, J = 7.7, 4.8 Hz, 1H), 6.87 (d, J = 8.7 Hz, 2H), 4.85 (s, 2H), 3.88-3.19 (m, 4H). ^{13}C NMR (100 MHz, DMSO-d_6) δ 197.4, 196.3, 162.0, 148.9, 148.3, 135.5, 133.0, 130.5, 127.9, 123.5, 115.2, 46.9, 37.5, 29.0. HRMS Calcd. For $C_{16}H_{17}N_2O_2S_2^+$ [M+H]$^+$ 333.0726, found: 333.0718.

4.2.5. 3-(4-Cyanophenyl)-3-oxopropyl (pyridin-3-ylmethyl)carbamodithioate (12) White solid, m.p. 146.7~147. 5 ^{o}C. Yield: 17%. ^{1}H NMR (400 MHz, DMSO-d_6) δ 10.51 (t, J = 5.5 Hz, 1H), 8.64-8.41 (m, 2H), 8.11 (d, J = 8.5 Hz, 2H), 8.00 (d, J = 8.5 Hz, 2H), 7.69 (d, J = 7.8 Hz, 1H), 7.36 (dd, J = 7.7, 4.8 Hz, 1H), 4.85 (d, J = 5.6 Hz, 2H), 3.52 (s, 4H). ^{13}C NMR (100 MHz, DMSO-d_6) δ 198.2, 197.7, 149.6, 148.9, 139.7, 136.0, 133.4, 133.3, 129.0, 124.0, 118.6, 115.8, 47.6, 39.1, 29.1. HRMS Calcd. For $C_{17}H_{16}N_3OS_2^+$ [M+H]$^+$ 342.0729, found: 342.0723.

4.2.6. 3-(4-Nitrophenyl)-3-oxopropyl (pyridin-3-ylmethyl)carbamodithioate (13) Light yellow solid, m.p. 153.0~154.1 ^{o}C. Yield: 27%. ^{1}H NMR (400 MHz, DMSO-d_6) δ 8.69-8.43 (m, 2H), 8.34 (d, J = 8.9 Hz, 2H), 8.25-8.09 (m, 2H), 7.71 (dd, J = 7.8, 1.7 Hz, 1H), 7.38 (dd, J = 7.8, 4.8 Hz, 1H), 4.86 (s, 2H), 3.54 (d, J = 15.1 Hz, 4H). ^{13}C NMR (100 MHz, DMSO-d_6) δ 197.5, 197.1, 150.0, 149.0, 148.3, 140.6, 135.5, 132.9, 129.3, 123.8, 123.5, 46.9, 38.8, 28.5. HRMS Calcd. For $C_{16}H_{16}N_3O_3S_2^+$ [M+H]$^+$ 362.0628, found: 362.0625.

4.2.7. 3-(4-(Dimethylamino)phenyl)-3-oxopropyl (pyridin-3-ylmethyl)carbamodithioate (14) White solid, m.p. 145.8~147.2 ^{o}C. Yield: 36%. ^{1}H NMR (400 MHz, DMSO-d_6) δ 10.46 (t, J = 5.3 Hz, 1H), 8.49 (dd, J = 11.1, 10.0 Hz, 2H), 7.75 (dd, J = 40.4, 8.4 Hz, 3H), 7.36 (dd, J = 7.7, 4.8 Hz, 1H), 6.71 (d, J = 8.9 Hz, 2H), 4.85 (d, J = 5.5 Hz, 2H), 3.49 (t, J = 6.7 Hz, 2H), 3.29 (t, J =

ACCEPTED MANUSCRIPT

6.7 Hz, 2H), 3.01 (s, 6H). ^{13}C NMR (100 MHz, DMSO-d_6) δ 197.6, 195.3, 153.3, 149.1, 148.4, 135.5, 133.0, 129.9, 123.8, 123.5, 110.7, 47.1, 39.6, 37.1, 29.4. HRMS Calcd. For $C_{18}H_{22}N_3OS_2^+$ [M+H]$^+$ 360.1199, found: 360.1197.

4.2.8. 3-(4-(Benzyloxy)phenyl)-3-oxopropyl (pyridin-3-ylmethyl)carbamodithioate (15) White solid, m.p. 148.3~148.9 °C. Yield: 22%. ^{1}H NMR (400 MHz, DMSO-d_6) δ 8.72-8.36 (m, 2H), 7.92 (dd, J = 9.4, 2.3 Hz, 2H), 7.69 (dt, J = 7.8, 1.9 Hz, 1H), 7.38 (dqd, J = 9.6, 8.7, 4.3 Hz, 6H), 7.11 (d, J = 8.9 Hz, 2H), 5.19 (s, 2H), 4.85 (s, 2H), 3.76-3.26 (m, 4H). ^{13}C NMR (100 MHz, DMSO-d_6) δ 197.8, 197.0, 162.8, 149.5, 148.8, 136.9, 136.0, 133.4, 130.7, 129.8, 129.0, 128.5, 128.2, 124.0, 115.2, 70.0, 47.4, 38.2, 29.5. HRMS Calcd. For $C_{23}H_{23}N_2O_2S_2^+$ [M+H]$^+$ 423.1196, found: 423.1194.

4.2.9. 3-(4-Methoxyphenyl)-3-oxopropyl (pyridin-3-ylmethyl)carbamodithioate (16) White solid, m.p. 135.5~135.8 °C. Yield: 54%. ^{1}H NMR (400 MHz, DMSO-d_6) δ 10.49 (t, J = 5.2 Hz, 1H), 8.50 (dd, J = 19.5, 2.4 Hz, 2H), 7.94 (d, J = 8.8 Hz, 2H), 7.70 (d, J = 7.8 Hz, 1H), 7.36 (dd, J = 7.7, 4.8 Hz, 1H), 7.03 (d, J = 8.8 Hz, 2H), 4.86 (d, J = 5.5 Hz, 2H), 3.84 (s, 3H), 3.44 (ddd, J = 17.6, 12.1, 5.6 Hz, 4H). ^{13}C NMR (100 MHz, DMSO-d_6) δ 197.9, 197.0, 163.7, 149.6, 148.9, 136.0, 133.4, 130.7, 129.7, 124.0, 114.4, 56.0, 47.6, 38.2, 29.5. HRMS Calcd. For $C_{17}H_{19}N_2O_2S_2^+$ [M+H]$^+$ 347.0883, found: 347.0876.

4.2.10. 3-Oxo-3-(4-(trifluoromethyl)phenyl)propyl (pyridin-3-ylmethyl)carbamodithioate (17) White solid, m.p. 135.8~136.6 °C. Yield: 11%. ^{1}H NMR (400 MHz, DMSO-d_6) δ 10.51 (t, J = 5.5 Hz, 1H), 8.69-8.43 (m, 2H), 8.16 (d, J = 8.1 Hz, 2H), 7.90 (d, J = 8.3 Hz, 2H), 7.71 (d, J = 1.8 Hz, 1H), 7.37 (dd, J = 7.8, 4.8 Hz, 1H), 4.85 (d, J = 5.6 Hz, 2H), 3.53 (s, 4H). ^{13}C NMR (100 MHz, DMSO-d_6) δ 198.3, 197.7, 149.6, 148.9, 139.7, 136.0, 133.4, 133.0, 129.2, 126.2, 124.0, 109.9, 47.6, 39.1, 29.1. HRMS Calcd. For $C_{17}H_{16}F_3N_2OS_2^+$ [M+H]$^+$ 385.0651, found: 385.0644.

4.2.11. 3-(2-Methoxyphenyl)-3-oxopropyl (pyridin-3-ylmethyl)carbamodithioate (18) White solid, m.p. 96.2~97.0 °C. Yield: 14%. ^{1}H NMR (400 MHz, DMSO-d_6) δ 10.47 (t, J = 5.5 Hz, 1H), 8.62-8.41 (m, 2H), 7.69 (dt, J = 7.8, 1.8 Hz, 1H), 7.64-7.46 (m, 2H), 7.36 (dd, J = 7.6, 4.7 Hz, 1H), 7.17 (d, J = 8.3 Hz, 1H), 7.11-6.97 (m, 1H), 4.85 (d, J = 5.6 Hz, 2H), 3.86 (s, 3H), 3.58-3.32 (m, 4H). ^{13}C NMR (100 MHz, DMSO-d_6) δ 199.9, 197.9, 158.9, 149.5, 148.9, 135.9, 134.5, 133.4, 130.0, 127.5, 124.0, 121.0, 113.0, 56.3, 47.5, 43.6, 29.4. HRMS Calcd. For $C_{17}H_{19}N_2O_2S_2^+$ [M+H]$^+$ 347.0883, found: 347.0877.

4.2.12. 3-(2-Chlorophenyl)-3-oxopropyl (pyridin-3-ylmethyl)carbamodithioate (19) White solid, m.p. 78.0~78.6 °C. Yield: 8%. ^{1}H NMR (400 MHz, DMSO-d_6) δ 10.53 (t, J = 5.4 Hz, 1H), 8.84-8.32 (m, 2H), 7.67 (dd, J = 9.9, 7.8 Hz, 2H), 7.58-7.33 (m, 4H), 4.85 (d, J = 5.6 Hz, 2H), 3.44 (dt, J = 12.9, 6.7 Hz, 4H). ^{13}C NMR (100 MHz, DMSO-d_6) δ 201.1, 197.5, 149.5, 148.9, 138.5, 135.9, 133.4, 132.9, 131.0, 130.1, 129.7, 128.0, 124.0, 47.6, 42.5, 29.0. HRMS Calcd. For $C_{16}H_{16}ClN_2OS_2^+$ [M+H]$^+$ 351.0387, found: 351.0382.

4.2.13. 3-(3,4-Dichlorophenyl)-3-oxopropyl (pyridin-3-ylmethyl)carbamodithioate (20) White solid, m.p. 139.3~140.2 °C. Yield: 56%. ^{1}H NMR (400 MHz, DMSO-d_6) δ 10.52 (q, J = 5.3 Hz, 1H), 8.77-8.28 (m, 2H), 8.37-8.05 (m, 1H), 7.92 (dd, J = 4.9, 3.5 Hz, 1H), 7.79 (td, J = 8.3, 4.1 Hz, 1H), 7.75-7.58 (m, 1H), 7.60-7.26 (m, 1H), 5.09-4.70 (m, 2H), 3.74-3.39 (m, 4H). ^{13}C NMR (100 MHz, DMSO-d_6) δ 197.2, 196.5, 149.1, 148.4, 136.2, 135.5, 132.9, 131.9, 131.1, 129.8, 127.9, 123.5, 47.1, 38.4, 28.6. HRMS Calcd. For $C_{16}H_{15}Cl_2N_2OS_2^+$ [M+H]$^+$ 384.9997, found: 384.9989.

4.2.14. 3-(3,4-Difluorophenyl)-3-oxopropyl (pyridin-3-ylmethyl)carbamodithioate (21) White solid, m.p. 128.8~129.7 °C. Yield: 25%. ^{1}H NMR (400 MHz, DMSO-d_6) δ 10.51 (s, J = 4.9 Hz, 1H), 8.62-8.35 (m, 2H), 7.99 (t, J = 8.2 Hz, 1H), 7.86 (d, J = 2.1 Hz, 1H), 7.70 (d, J = 7.8 Hz, 1H), 7.56 (d, J = 5.1 Hz, 1H), 7.42-7.28 (m, 1H), 4.86 (d, J = 5.4 Hz, 2H), 3.49 (tt, J = 8.4, 4.2 Hz, 4H). ^{13}C NMR (100 MHz, DMSO-d_6) δ 207.2, 196.6, 151.1, 149.7, 149.5, 149.0, 148.6, 136.1, 135.8, 134.1, 133.4, 124.0, 117.8, 47.5, 38.8, 29.2. HRMS Calcd. For $C_{16}H_{15}F_2N_2OS_2^+$ [M+H]$^+$ 353.0588, found: 353.0581.

4.2.15. 3-Oxo-3-(3,4,5-trimethoxyphenyl)propyl (pyridin-3-ylmethyl)carbamodi- thioate (22) White solid, m.p. 85.6~86.8 °C. Yield: 46%. ^{1}H NMR (400 MHz, DMSO-d_6) δ 10.52 (s, J = 5.0 Hz, 1H), 8.49 (dd, J = 11.1, 10.2 Hz, 2H), 7.70 (d, J = 7.8 Hz, 1H), 7.37 (dd, J = 7.6, 4.9 Hz, 1H), 7.23 (d, J = 28.6 Hz, 2H), 4.86 (d, J = 5.4 Hz, 2H), 3.85 (s, 6H), 3.74 (s, 3H), 3.61-3.40 (m, 4H). ^{13}C NMR (100 MHz, DMSO-d_6) δ 197.4, 197.2, 152.8, 149.1, 148.4, 142.0, 135.5, 132.9, 131.5, 123.5, 105.4, 60.1, 56.0, 47.1, 38.1, 29.1. HRMS Calcd. For $C_{19}H_{23}N_2O_4S_2^+$ [M+H]$^+$ 407.1094, found: 407.1087.

4.2.16. 3-(Naphthalen-2-yl)-3-oxopropyl (pyridin-3-ylmethyl)carbamodithioate (23) White solid, m.p. 137.0~139.4 °C. Yield: 33%. ^{1}H NMR (400 MHz, DMSO-d_6) δ 10.55 (s, 1H), 8.70 (s, 1H), 8.62-8.43 (m, 2H), 8.14 (d, J = 7.7 Hz, 1H), 8.01 (s, 3H), 7.81-7.56 (m, 3H), 7.37 (dd, J = 7.6, 4.8 Hz, 1H), 4.89 (s, 2H), 3.63 (s, 4H). ^{13}C NMR (100 MHz, DMSO-d_6) δ 198.1, 197.4, 149.1, 148.4, 135.5, 135.1, 133.4, 132.9, 132.2, 130.0, 129.6, 128.7, 128.3, 127.6, 126.9, 123.5, 123.3, 47.1, 38.3, 29.0. HRMS Calcd. For $C_{20}H_{19}N_2OS_2^+$ [M+H]$^+$ 367.0933, found: 367.0928.

4.2.17. 3-(Naphthalen-1-yl)-3-oxopropyl (pyridin-3-ylmethyl)carbamodithioate (24) White solid, m.p. 107.2~108.7 °C. Yield: 32%. ^{1}H NMR (400 MHz, DMSO-d_6) δ 10.61 (t, J = 5.5 Hz, 1H), 8.63-8.44 (m, 3H), 8.14 (d, J = 8.2 Hz, 1H), 8.08 (d, J = 7.2 Hz, 1H), 8.05-7.99 (m, 1H), 7.74 (d, J = 7.8 Hz, 1H), 7.68-7.52 (m, 3H), 7.37 (dd, J = 7.8, 4.8 Hz, 1H), 4.92 (d, J = 5.5 Hz, 2H), 3.64 (qd, J = 7.7, 1.2 Hz, 4H). ^{13}C NMR (100 MHz, DMSO-d_6) δ 202.2, 197.3, 149.1, 148.4, 135.5, 134.7, 133.5, 132.9, 132.7, 129.3, 128.5, 128.3, 127.9, 126.4, 125.2, 124.8, 123.5, 47.2, 41.3, 29.3. HRMS Calcd. For $C_{20}H_{19}N_2OS_2^+$ [M+H]$^+$ 367.0933, found: 367.0933.

4.2.18. 3-(Furan-2-yl)-3-oxopropyl (pyridin-3-ylmethyl)carbamodithioate (25) White solid, m.p. 122.9~123.6 °C. Yield: 64%. ^{1}H NMR (400 MHz, DMSO-d_6) δ 10.51 (t, J = 5.5 Hz, 1H), 8.82-8.26 (m, 2H), 7.99 (dd, J = 1.6, 0.6 Hz, 1H), 7.69 (dt, J = 7.8, 1.9 Hz, 1H), 7.60-7.18 (m, 2H), 6.71 (dd, J = 3.6, 1.7 Hz, 1H), 4.85 (d, J = 5.6 Hz, 2H), 3.49 (t, J = 6.8 Hz, 2H), 3.26 (t, J =

ACCEPTED MANUSCRIPT

6.8 Hz, 2H). ^{13}C NMR (100 MHz, DMSO-d_6) δ 197.5, 186.9, 152.1, 149.6, 148.9, 148.4, 136.0, 133.4, 124.0, 119.1, 113.0, 47.6, 38.2, 29.0. HRMS Calcd. For $C_{14}H_{15}N_2O_2S_2^+$ $[M+H]^+$ 307.0570, found: 307.0563.

4.2.19. 3-Oxo-3-(thiophen-2-yl)propyl (pyridin-3-ylmethyl)carbamodithioate (26) White solid, m.p. 135.3~136.2 °C. Yield: 53%. ^{1}H NMR (400 MHz, DMSO-d_6) δ 10.49 (t, J = 5.3 Hz, 1H), 8.56-8.45 (m, 2H), 8.02 (dd, J = 4.9, 1.1 Hz, 1H), 7.96 (dd, J = 3.8, 1.1 Hz, 1H), 7.69 (dt, J = 7.8, 1.8 Hz, 1H), 7.37 (ddd, J = 7.8, 4.8, 0.7 Hz, 1H), 7.24 (dd, J = 4.9, 3.8 Hz, 1H), 4.85 (d, J = 5.6 Hz, 2H), 3.51 (t, J = 6.5 Hz, 2H), 3.39 (dd, J = 10.3, 3.6 Hz, 2H). ^{13}C NMR (100 MHz, DMSO-d_6) δ 197.6, 191.7, 149.6, 148.9, 143.7, 136.0, 135.5, 134.0, 133.4, 129.3, 124.0, 47.6, 38.9, 29.4. HRMS Calcd. For $C_{14}H_{15}N_2OS_3^+$ $[M+H]^+$ 323.0341, found: 323.0339.

4.2.20. 3-Oxo-3-(1H-pyrrol-2-yl)propyl (pyridin-3-ylmethyl)carbamodithioate (27) White solid, m.p. 128.7~129.3 °C. Yield: 19%. ^{1}H NMR (400 MHz, DMSO-d_6) δ 11.85 (s, 1H), 10.47 (t, J = 5.3 Hz, 1H), 8.57-8.39 (m, 2H), 7.69 (d, J = 7.8 Hz, 1H), 7.36 (dd, J = 7.7, 4.8 Hz, 1H), 7.09 (s, 1H), 6.97 (s, 1H), 6.22-6.13 (m, 1H), 4.86 (d, J = 5.5 Hz, 2H), 3.50 (t, J = 6.8 Hz, 2H), 3.18 (t, J = 6.9 Hz, 2H). ^{13}C NMR (100 MHz, DMSO-d_6) δ 197.8, 187.8, 149.6, 148.9, 136.0, 133.4, 131.8, 126.1, 124.0, 117.2, 110.3, 47.6, 37.6, 29.9. HRMS Calcd. For $C_{14}H_{16}N_3OS_2^+$ $[M+H]^+$ 306.0729, found: 306.0724.

4.2.21. 3-Oxo-3-(thiazol-2-yl)propyl (pyridin-3-ylmethyl)carbamodithioate (28) Yellow solid, m.p. 114.0~114.9 °C. Yield: 10%. ^{1}H NMR (400 MHz, $CDCl_3$) δ 9.12-8.96 (m, 1H), 8.51-8.36 (m, 2H), 8.02-7.93 (m, 1H), 7.70 (dd, J = 7.1, 4.2 Hz, 2H), 7.28-7.20 (m, 1H), 5.03-4.89 (m, 2H), 3.77-3.62 (m, 4H). ^{13}C NMR (100 MHz, $CDCl_3$) δ 198.2, 191.9, 166.2, 149.2, 148.8, 144.9, 136.3, 132.6, 126.6, 123.8, 48.1, 38.9, 29.0. HRMS Calcd. For $C_{13}H_{14}N_3OS_3^+$ $[M+H]^+$ 324.0294, found: 324.0290.

4.2.22. 3-Oxo-3-(pyridin-3-yl)propyl (pyridin-3-ylmethyl)carbamodithioate (29) Yellow solid, m.p. 95.1~195.9 °C. Yield: 11%. ^{1}H NMR (400 MHz, DMSO-d_6) δ 10.52 (t, J = 5.3 Hz, 1H), 9.13 (t, J = 4.3 Hz, 1H), 8.80 (dd, J = 4.7, 1.4 Hz, 1H), 8.50 (dd, J = 20.1, 2.4 Hz, 2H), 8.30 (dd, J = 6.1, 1.8 Hz, 1H), 7.70 (d, J = 7.8 Hz, 1H), 7.56 (dd, J = 7.8, 4.8 Hz, 1H), 7.36 (dd, J = 7.7, 4.8 Hz, 1H), 4.86 (d, J = 5.5 Hz, 2H), 3.53 (t, J = 4.3 Hz, 4H). ^{13}C NMR (100 MHz, DMSO-d_6) δ 198.3, 197.7, 154.1, 149.6, 149.6, 148.9, 136.0, 135.9, 133.4, 131.9, 124.4, 124.0, 47.6, 39.0, 29.1. HRMS Calcd. For $C_{15}H_{16}N_3OS_2^+$ $[M+H]^+$ 318.0729, found: 318.0725.

4.2.23. 3-Oxo-3-(2-oxo-2H-chromen-3-yl)propyl (pyridin-3-ylmethyl)carbamodithioate (30) White solid, m.p. 127.8~128.7 °C. Yield: 6%. ^{1}H NMR (400 MHz, DMSO-d_6) δ 10.49 (t, J = 5.5 Hz, 1H), 8.75-8.68 (m, 1H), 8.54-8.42 (m, 2H), 7.98 (dd, J = 7.8, 1.2 Hz, 1H), 7.74 (ddd, J = 22.0, 12.9, 4.6 Hz, 2H), 7.50-7.34 (m, 3H), 4.85 (d, J = 5.6 Hz, 2H), 3.58-3.37 (m, 4H). ^{13}C NMR (100 MHz, DMSO-d_6) δ 197.7, 196.1, 158.8, 155.1, 149.6, 148.9, 147.9, 136.0, 135.1, 133.4, 131.3, 125.4, 124.3, 124.0, 118.6, 116.6, 47.6, 42.4, 29.0. HRMS Calcd. For $C_{19}H_{17}N_2O_3S_2^+$ $[M+H]^+$ 385.0675, found: 385.0672.

4.2.24. 3-(1H-indol-3-yl)-3-oxopropyl (pyridin-3-ylmethyl)carbamodithioate (31) White solid, m.p. 156.6~157.4 °C. Yield: 6%. ^{1}H NMR (400 MHz, DMSO-d_6) δ 11.96 (s, 1H), 10.45 (t, J = 5.5 Hz, 1H), 8.56-8.45 (m, 2H), 8.33 (d, J = 3.1 Hz, 1H), 8.25-8.13 (m, 1H), 7.75-7.63 (m, 1H), 7.47 (dd, J = 6.7, 1.7 Hz, 1H), 7.37 (dd, J = 7.8, 4.8 Hz, 1H), 7.26-7.12 (m, 2H), 4.86 (d, J = 5.6 Hz, 2H), 3.55 (t, J = 6.9 Hz, 2H), 3.29 (t, J = 7.0 Hz, 2H). ^{13}C NMR (100 MHz, DMSO-d_6) δ 198.1, 193.4, 149.6, 148.9, 137.1, 135.9, 134.5, 133.5, 125.8, 124.0, 123.3, 122.3, 121.7, 116.5, 112.6, 47.5, 38.8, 30.0. HRMS Calcd. For $C_{18}H_{18}N_3OS_2^+$ $[M+H]^+$ 356.0886, found: 356.0883.

4.2.25. The preparation of compound 32

1-(1H-pyrrolo[2,3-b]pyridin-3-yl)ethan-1-one (36)[27], ^{1}H NMR (400 MHz, $CDCl_3$) δ 13.11-12.78 (m, 1H), 8.79-8.69 (m, 1H), 8.47-8.37 (m, 1H), 8.15-7.98 (m, 1H), 7.36-7.28 (m, 1H), 2.64-2.52 (m, 3H).

3-Oxo-3-(1H-pyrrolo[2,3-b]pyridin-3-yl)propyl (pyridin-3-ylmethyl)carbamodithioate (32) White solid, m.p. 147.8~148.2 °C. Yield: 12%. ^{1}H NMR (400 MHz, DMSO-d_6) δ 12.50 (s, 1H), 10.47 (t, J = 5.5 Hz, 1H), 8.56-8.43 (m, 4H), 8.33 (dd, J = 4.7, 1.6 Hz, 1H), 7.74-7.65 (m, 1H), 7.37 (dd, J = 7.7, 4.8 Hz, 1H), 7.26 (dd, J = 7.9, 4.7 Hz, 1H), 4.86 (d, J = 5.6 Hz, 2H), 3.55 (t, J = 6.8 Hz, 2H), 3.31 (d, J = 7.0 Hz, 2H). ^{13}C NMR (100 MHz, DMSO-d_6) δ 198.0, 193.6, 149.6, 149.4, 148.9, 144.7, 135.9, 134.9, 133.4, 130.0, 124.0, 118.6, 118.1, 115.1, 47.6, 38.7, 29.8. HRMS Calcd. For $C_{17}H_{17}N_4OS_2^+$ $[M+H]^+$ 357.0838, found: 357.0832.

4.2.26. The preparation of compound 33

1-(Imidazo[1,2-a]pyridin-3-yl)ethan-1-one (37)[28], ^{1}H NMR (400 MHz, $CDCl_3$) δ 9.73-9.47 (m, 1H), 8.46-8.27 (m, 1H), 7.88-7.69 (m, 1H), 7.56-7.42 (m, 1H), 7.25-6.94 (m, 1H), 2.86-2.35 (m, 3H).

3-(Imidazo[1,2-a]pyridin-3-yl)-3-oxopropyl (pyridin-3-ylmethyl)carbamodithioate (33) White solid, m.p. 164.8~165.6 °C. Yield: 14%. ^{1}H NMR (400 MHz, DMSO-d_6) δ 10.51 (t, J = 5.1 Hz, 1H), 9.54 (d, J = 6.8 Hz, 1H), 8.64 (s, 1H), 8.50 (dd, J = 10.4, 8.8 Hz, 3H), 7.85 (d, J = 8.9 Hz, 1H), 7.70 (d, J = 7.7 Hz, 1H), 7.38 (d, J = 5.0 Hz, 1H), 7.29 (t, J = 6.7 Hz, 1H), 4.86 (d, J = 5.0 Hz, 2H), 3.59 (t, J = 6.8 Hz, 2H), 3.40 (t, J = 6.8 Hz, 2H). ^{13}C NMR (100 MHz, DMSO-d_6) δ 197.1, 187.6, 149.1, 148.4, 143.8, 135.5, 132.9, 132.6, 129.6, 128.0, 123.5, 123.0, 117.4, 115.6, 47.1, 38.3, 29.3. HRMS Calcd. For $C_{17}H_{17}N_4OS_2^+$ $[M+H]^+$ 357.0838, found: 357.0832.

4.2.27. 3-Oxo-5-phenylpent-4-en-1-yl (pyridin-3-ylmethyl)carbamodithioate (34) White solid, m.p. 119.9~120.6 °C. Yield: 28 %. ^{1}H NMR (400 MHz, DMSO-d_6) δ 10.50 (t, J = 5.4 Hz, 1H), 8.64-8.36 (m, 2H), 7.77-7.61 (m, 4H), 7.47-7.34 (m, 4H), 6.91 (d, J = 16.3 Hz, 1H), 4.86 (d, J = 5.6 Hz, 2H), 3.47 (t, J = 6.7 Hz, 2H), 3.16 (t, J = 6.8 Hz, 2H). ^{13}C NMR (100 MHz, DMSO-d_6) δ 198.1, 197.3, 149.1, 148.4, 142.6, 135.5, 134.3, 132.9, 130.5, 128.9, 128.5, 126.1, 123.5, 47.1, 39.9, 28.7. HRMS Calcd. For $C_{18}H_{19}N_2OS_2^+$ $[M+H]^+$ 343.0933, found: 367.0930.

4.2.28 3-Oxo-3-(1H-pyrrol-3-yl)propyl (pyridin-3-ylmethyl)carbamodithioate (35) White solid, m.p. 145.5~146.8 °C. Yield: 24 %. ^{1}H NMR (400 MHz, DMSO-d_6) δ 11.47 (s, 1H), 10.45 (t, J = 5.5 Hz, 1H), 8.65-8.32 (m, 2H), 7.84-7.62 (m, 1H), 7.59 (dt, J = 3.1, 1.6 Hz, 1H), 7.37 (dd, J = 7.8, 4.8 Hz, 1H), 6.83 (dd, J =

ACCEPTED MANUSCRIPT

4.6, 2.4 Hz, 1H), 6.45 (dd, *J* = 4.1, 2.5 Hz, 1H), 4.85 (d, *J* = 5.6 Hz, 2H), 3.46 (t, *J* = 6.9 Hz, 2H), 3.14 (t, *J* = 6.9 Hz, 2H). ^{13}C NMR (100 MHz, DMSO-d_6) δ 198.1, 193.1, 149.6, 148.9, 135.9, 133.5, 125.1, 124.8, 124.0, 120.4, 107.9, 47.5, 38.8, 29.8. HRMS Calcd. For $C_{14}H_{16}N_3OS_2^+$ $[M+H]^+$ 305.0708, found: 367.0728.

4.3. Purification of recombinant pyruvate kinase isoforms

The human cDNA for PKM2, PKM1 and PKR were cloned into pET28a with a N-terminal His tag and purified from *E.coli* strain BL21 (Invitrogen) using Ni-Agarose beads (Qiagen) as described previously.[12] Briefly, *E.coli* grown to an OD (600 nm) of 0.6 were induced with 0.5 mM IPTG at 21 ℃ for 4 h. Cells were collected and lysed by freeze/thaw cycles and sonication. Lysate was passed over a Ni-NTA agarose column and eluted with 250 mM imidazole in 1 ml fractions. Fractions with high concentration of pyruvate kinase were determined using SDS-PAGE and coomassie staining according to standard protocol.

4.4. Measurement of enzyme activity

Fluorescent Pyruvate Kinase-Lactate Dehydrogenase Coupled Assay. All compounds were tested in a kinetic mode by coupling the generation of pyruvate by pyruvate kinase to the depletion of NADH through lactate dehydrogenase.[34] For PKM2, 45 μL of substrate mix (final concentration, 50 mM Tris-Cl pH 8.0, 200 mM KCl, 15 mM $MgCl_2$, 0.1 mM PEP, 4.0 mM ADP and 0.2 mM NADH) was dispensed into Corning black solid 96-well plates and 1 uL of compounds were delivered using a Eppendorf pin tool and then 5 μL of enzyme mix (final concentrations, 10 nM hPKM2 and 1 μM of LDH) was added. Plates were immediately placed in FlexStation 3 (Molecular Devices), and NADH fluorescence was determined at 30 s exposure intervals for between 3 and 6 min. Data were normalized to the untreated and AC_{100} activation using known activators such as FBP. Data was fit in GraphPad prism. Conversion of fluorescent units to pmols of NADH was performed using a standard curve of known NADH concentrations. Data was collected on the FlexStation 3.

4.5. In vitro anti-proliferative Assay

The in vitro anti-proliferation of the chemical compounds was measured by the MTT reagent, as described in the literature[35]. Briefly, 5×10^3 cells in 100 μL of medium per well were plated in 96-well plates. After incubated for 24 h, the cells were treated with different concentration of tested compound or DMSO (as negative control) for 48 h. Then the medium with compound or DMSO was replaced with 200 μL of fresh medium containing 10 % MTT (5 mg/mL in PBS) in each well and incubated at 37 °C for 4 h. Last, the MTT-containing medium was discarded and 150 μL of DMSO per well was added to dissolve the formazan crystals newly formed. Absorbance of each well was determined by a microplate reader (Flexstation 3) at a 570 nm wavelength. The inhibition rates of proliferation were calculated with the following equation:

$$Inhibition(\%) = \frac{OD(DMSO) - OD(compd)}{OD(DMSO) - OD(blank)} \times 100$$

4.6. Cell cycle analysis.

Cell cycle status was detected by flow cytometry according to a previously published method[36] and was analyzed by Flow Jo 4.0. Briefly, cells were first treated with DMSO or different concentrations of compound **32** for 12 h and then harvested, washed twice with 1 × PBS, and resuspended in 200 μL of 1 × PBS. The cells were fixed in 4 mL of ice-cold 75 % ethanol at −20 °C overnight and stained with 500 μL of propidium iodide (50 μg/mL, Sigma) containing 0.1 % RNase (1 mg/mL, Sigma) for 15 min in dark conditions at room temperature. The cells were then analyzed by flow cytometry (FACSVerse™, BD). The results were indicated as mean values from three independent determinations.

4.7. Procedures for molecular docking:

Molecular docking was carried out by using AutoDock 4.2 (Scripps Research Institute),[37] assessed by OpenSource PyMOL 1.3.x (Schrödinger, LLC) and PoseView web service (Universität Hamburg) afterwards.[38] The X-ray crystal structure of PKM2 and its reported activator compound 4 (NZT) taken from PDB (4G1N) was used as the input structure. Receptor preparation: All HETATM and hydrogen atoms are deleted and crystal cell is removed. Alternative conformers of residues are also deleted to retain one set. Then the receptor is further processed via AutoDock Tools 1.5.6 rc3. Polar hydrogen and Kollman charge is added to finally give the prepared protein. Ligand preparation: Polar hydrogen and Gasteiger charge is given and there is no further modifications on the ligand torsion tree. Molecular docking: Parameter selection is done via AutoDock Tools 1.5.6 rc3. Whilst other parameters for AutoDock were set as default, the Number of GA Run was modified to 100 for reliability and accuracy reasons.

Acknowledgments

We gratefully acknowledge the generous support provided by The National Natural Science Funds of China (No. 21172011，81372491, 81430056, 31420103905 & 81321003) and the 111 Project (B07001).

References and notes

1. Warburg, O. *Science*, **1956**, 123, 309.
2. Kroemer, G.; Pouyssegur, *J. Cancer. Cell.* **2008**, 13, 472.
3. Vander Heiden, M. G.; Cantley, L. C.; Thompson, C. B. *Science*, **2009**, 324, 1029.
4. Tani, K.; Yoshida, M. C.; Satoh, H.; Mitamura, K.; Noguchi, T.; Tanaka, T.; Fujii, H.; Miwa, S. *Gene*, **1988**, 73, 509.
5. Takenaka, M.; Yamada, K.; Lu, T.; Kang, R.; Tanaka, T.; Noguchi, T. Eur. *J. Biochem.* **1996**, 235, 366.
6. Noguchi, T.; Inoue, H.; Tanaka, T. *J. Biol. Chem.* **1986**, 261, 13807.
7. Noguchi, T.; Yamada, K.; Inoue, H.; Matsuda, T.; Tanaka, T. *J. Biol. Chem.* **1987**, 262, 14366.
8. Ashizawa, K.; Willingham, M. C.; Liang, C.; Cheng, S. *J. Biol. Chem.* **1991**, 266, 16842.
9. Dombrauckas, J. D.; Santarsiero, B. D.; Mesecar, A. D. *Biochemistry*, **2005**, 44, 9417.
10. Hathurusinghe, H. R.; Goonetilleke, K. S.; Siriwardena, A. K. Ann. Surg. *Oncol*. **2007**, 14, 2714.
11. Mazurek, S. Int. J. Biochem. *Cell Biol.* **2011**, 43, 969.
12. Christofk, H. R.; Heiden, M. G. V.; Harris, M. H.; Ramanathan, A.; Gerszten, R. E.; Wei, R.; Fleming, M. D.; Schreiber, S. L.; Cantley, L. C. *Nature*, **2008**, 452, 230.
13. Yang, W.; Zheng, Y.; Xia, Y.; Ji, H.; Chen, X.; Guo, F.; Lyssiotis, C. A.; Aldape, K.; Cantley, L. C.; Lu, Z. Nat. *Cell Biol*. **2012**, 14, 1295.
14. Yang, W.; Xia, Y.; Ji, H.; Zheng, Y.; Liang, J.; Huang, W.; Gao, X.; Aldape, K.; Lu, Z. *Nature*, **2011**, 480, 118.
15. Gao, X.; Wang, H.; Yang, J.; Liu, X.; Liu, Z. *Mol. Cell*, **2012**, 45, 598.
16. Luo, W.; Hu, H.; Chang, R.; Zhong, J.; Knabel, M.; O'Meally, R.; Cole, R. N.; Pandey, A.; Semenza, G. L. *Cell*, **2011**, 145, 732.
17. Boxer, M. B.; Jiang, J.; Heiden, M. G. V.; Shen, M.; Skoumbourdis, A. P.; Southall, N.; Veith, H.; Leister, W.; Austin, C. P.; Park, H. W.;

ACCEPTED MANUSCRIPT

Inglese, J.; Cantley, L. C.; Auld, D. S.; Thomas, C. J. *J. Med. Chem.* **2010**, 53, 1048.
18. Jiang, J. K.; Boxer, M. B.; Vander Heiden, M. G.; Shen, M.; Skoumbourdis, A. P.; Southall, N.; Veith, H.; Leister, W.; Austin, C. P.; Park, H. W.; Inglese, J.; Cantley, L. C.; Auld, D. S.; Thomas, C. J. *Bioorg. Med. Chem. Lett*. **2010**, 20, 3387.
19. Walsh, M. J.; Brimacombe, K. R.; Veith, H.; Bougie, J. M.; Daniel, T.; Leister, W.; Cantley, L. C.; Israelsen, W. J.; Heiden, M. G. V.; Shen, M.; Auld, D. S.; Thomas, C. J.; Boxer, M. B. *Bioorg. Med. Chem. Lett.* **2011**, 21, 6322.
20. Kung, C.; Hixon, J.; Choe, S.; Marks, K.; Gross, S.; Murphy, E.; DeLaBarre, B.; Cianchetta, G.; Sethumadhavan, S.; Wang, X.; Yan, S.; Gao, Y.; Fang, C.; Wei, W.; Jiang, F.; Wang, S.; Qian, K.; Saunders, J.; Driggers, E.; Woo, H. K.; Kunii, K.; Murray, S.; Yang, H.; Yen, K.; Liu, W.; Cantley, L. C.; Heiden, M. G. V.; Su, S.; Jin, S.; Salituro, F. G.; Dang, L. *Chem. Biol.* **2012**, 19, 1187.
21. Yacovan, A.; Ozeri, R.; Kehat, T.; Mirilashvili, S.; Sherman, D.; Aizikovich, A.; Shitrit, A.; Ben-Zeev, E.; Schutz, N.; Bohana-Kashtan, O.; Konson, A.; Behar, V.; Becker, O. M. *Bioorg. Med. Chem. Lett.* **2012**, 22, 6460.
22. Guo, C.; Linton, A.; Jalaie, M.; Kephart, S.; Ornelas, M.; Pairish, M.; Greasley, S.; Richardson, P.; Maegley, K.; Hickey, M.; Li, J.; Wu, X.; Ji, X.; Xie, Z. *Bioorg. Med. Chem. Lett.* **2013**, 23, 3358.
23. Xu, Y.; Liu, X.; Saunders, M.; Pearce, S.; Foulks, J. M.; Parnell, K. M.; Clifford, A.; Nix, R. N.; Bullough, J.; Hendrickson, T. F.; Wright, K.; McCullar, M. V.; Kanner, S. B.; Ho, K. K. *Bioorg. Med. Chem. Lett.* **2014**, 24, 515.
24. Li, Y.; Wang, Z.; Yan, X.; Chen, M.; Bao, J.; Wu, G.; Ge, Z.; Zhou, D.; Wang, Y.; Li, R. *Cancer Lett.* **2013**, 340, 88.
25. Bugarin, A.; Jones, K. D.; Connell, B. T. *Chem. Commun.* **2010**, 46, 1715.
26. Guo, B.; Ge, Z.; Cheng, T.; Li, R. *Synth. Commun*. **2001**, 31, 3021.
27. Zhang, Z.; Yang, Z.; Wong, H.; Zhu, J.; Meanwell, N. A.; Kadow, J. F.; Wang, T. *J. Org. Chem.* **2002**, 67, 6226.
28. Hayakawa, M.; Kaizawa, H.; Kawaguchi, K.; Ishikawa, N.; Koizumi, T.; Ohishi, T.; Yamano, M.; Okada, M.; Ohta, M.; Tsukamoto, S.; Raynaud, F. I.; Waterfield, M. D.; Parker, P.; Workman, P. *Bioorg. Med. Chem.* **2007**, 15, 403.
29. Parnell, K. M.; Foulks, J. M.; Nix, R. N.; Clifford, A.; Bullough, J.; Luo, B.; Senina, A.; Vollmer, D.; Liu, J.; McCarthy, V.; Xu, Y.; Saunders, M.; Liu, X. H.; Pearce, S.; Wright, K.; O'Reilly, M.; McCullar, M. V.; Ho, K. K.; Kanner, S. B. *Mol. Cancer. Ther*, **2013**, 12, 1453.
30. Safavy, A.; Raisch, K. P.; Khazaeli, M. B.; Buchsbaum, D. J.; Bonner, J. A. *J. Med. Chem.* **1999**, 42, 4919.
31. Mahboobi, S.; Pongratz, H.; Hufsky, H.; Hockemeyer, J.; Frieser, M.; Lyssenko, A.; Paper, D. H.; Burgermeister, J.; Bohmer, F. D.; Fiebig, H. H.; Burger, A. M.; Baasner, S.; Beckers, T. *J. Med. Chem.* **2001**, 44, 4535.
32. Jiang, Y.; Li, X.; Yang, W.; Hawke, D. H.; Zheng, Y.; Xia, Y.; Aldape, K.; Wei, C.; Guo, F.; Chen, Y.; Lu, Z. *Mol. Cell.* **2014**, 53, 75.
33. Jiang, Y.; Wang, Y.; Wang, T.; Hawke, D. H.; Zheng, Y.; Li, X.; Zhou, Q.; Majumder, S.; Bi, E.; Liu, D. X.; Huang, S.; Lu, X. *Nat. Commun.* **2014**, 5, 5566.
34. Hannaert, V.; Yernaux, C.; Rigden, D. J.; Fothergill-Gilmore, L. A.; Opperdoes, F. R.; Michels, *P. A. FEBS. Lett.* **2002**, 514, 255.
35. Zhou, W.; Zhang, X.; Xiao, L.; Ding, J.; Liu, Q. H.; Li, S. S. *Eur. J. Med. Chem.* **2011**, 46, 3420.
36. Yang, G.; Rosen, D. G.; Liu, G.; Yang, F.; Guo, X.; Xiao, X.; Xue, F.; Mercado-Uribe, I.; Huang, J.; Lin, S. H.; Mills, G. B.; Liu, *J. Clin. Cancer. Res.* **2010**, 16, 3875.
37. Morris, G. M.; Huey, R.; Lindstrom, W.; Sanner, M. F.; Belew, R. K.; Goodsell, D. S.; Olson, A. J. *J. Comput. Chem.* **2009**, 30, 2785.
38. Stierand, K.; Maass, P. C.; Rarey, M. *Bioinformatics*, **2006**, 22, 1710.

Supplementary Material

^{1}H NMR and ^{13}C NMR spectra for all the compounds and additional data and software were available in supporting information.

ACCEPTED MANUSCRIPT